Original Article

Anti-proliferative of Phenyl isoserine derivative containing 1,2,3-triazole ring on breast cancer cell line

Nawar Raad Hussein[1, 2*], Hayder Bahaa Sahib[3], Zahraa Sabbar Omran[4]

[1]Department of Pharmacology and Toxicology, College of Medicine, AL-Nahrain University, Iraq. [2]College of Pharmacy, Al-Farahidi University, Bagdad, Iraq. [3]Department of Pharmacology and Toxicology, College of Pharmacy, AL-Nahrain University, Bagdad, Iraq. [4]Department of Biochemistry, College of Medicine, Kerbala University, Karbala, Iraq.

Correspondence: Nawar Raad Hussein, Department of Pharmacology and Toxicology, College of Medicine, AL-Nahrain University, Iraq. ph.nawar@gmail.com

ABSTRACT

This work is crucial for investigating the antiproliferative effect of a phenyl isoserine derivative. The action of the phenyl isoserine derivative was estimated utilizing the *ex vivo* rat aorta ring (RAR) assay, cytotoxicity assay on human breast cancer cell line MCF-7, gene expression analysis for Vascular endothelial growth factor (VEGF) by real-time PCR, ADME/Tox profiling, and molecular docking studies. The findings indicated that the phenyl isoserine derivative had considerable antiangiogenic action in a dose-dependent fashion in the RAR assay. The phenyl isoserine derivative had an inhibiting effect on MCF-7 cells. The phenyl isoserine derivative exhibited a decrease in VEGF gene expression as identified by quantitative real-time PCR. ADME/Tox experiments demonstrated appropriate pharmacokinetic characteristics and predicted how well the docked medication will attach to the protein and forecasted the binding affinity of docked medication. This work shows that the phenyl isoserine derivative markedly reduces angiogenesis and suppresses VEGF activity, which is advantageous for tumor therapy.

Keywords: Phenyl isoserine derivative, Antiangiogenic activity, Breast cancer cell MCF-7, Molecular docking, VEGF gene expression

Introduction

Cancer is a critical health concern marked by the capacity to metastasize to adjacent tissues, the rapid proliferation of unregulated cells, and considerable morbidity and mortality [1]. The American Cancer Society reports that prostate and breast cancers constitute almost 12% of all cancer fatalities, with an anticipated 433,360 new cancer cases in 2018. Notwithstanding advancements in diagnostic and therapeutic approaches, these tumors in both genders typically have a bleak prognosis [2].

Angiogenesis is a crucial process in certain physiological settings, including wound healing, development, and the way the reproduction systems of women work. A number of disorders are caused by disruptions in the physiological angiogenesis pathways, manifesting as excessive angiogenesis in conditions such as retinopathies, arthritis, psoriasis, atherosclerosis, and cancers [3].

Triazole derivatives are highly recommended molecules in drug development and medical chemistry. Numerous investigations elucidated the potential of triazoles as novel agents for anticancer, anti-inflammatory, antifungal, and herbicidal applications. The development of a series of triazoles facilitated the suppression of VEGFR1 progression [4]. The acknowledged anticancer efficacy of these compounds is contingent upon their cellular incorporation rate and is directly correlated with hydrophilicity. Both qualities are influenced by the presence or absence of substituent hydroxyl groups, 1,2,3-triazoles, methyl groups, and nucleosides and by the length of acetamido or carboxylate groups [5].

Recent advancements in click chemistry are evident, with several published synthetic methods for the formulation of 1,2,3-triazole scaffolds. Numerous reviews have identified the click reaction as crucial in various domains, such as polymer grafting [6]. The

Access this article online	
Website: www.japer.in	**E-ISSN:** 2249-3379

How to cite this article: Hussein NR, Sahib HB, Omran ZS. Anti-proliferative of Phenyl isoserine derivative containing 1,2,3-triazole ring on breast cancer cell line. J Adv Pharm Educ Res. 2024;14(2):110-9. https://doi.org/10.51847/xHUGpvrkc9

production of 1,2,3-triazole scaffolds [7] and chemical ligation [8]. Recent publications have announced advancements in the development of peptidomimetics, bioconjugations, and surface chemistry [9].

This work aims to investigate the anti-angiogenic and anti-proliferative characteristics of a vanillin derivative with a 1,2,3-triazole ring and N-Benzoyl-3-phenyl isoserine. Utilizing the Aortic ring test, cytotoxicity assay, quantitative polymerase chain response in real time to measure gene utterance, molecular docking, and ADME estimation for pharmacokinetic parameters and targeted predictions, the substances exhibit anti-proliferative and anti-angiogenic properties.

Materials and Methods

This study was performed at the Department of Pharmacology, College of Medicine, Al-Nahrain University, from December 1, 2022, until July 1, 2023. All experimental procedures complied with the standards set by Animal Care and received approval from The Research Ethical Committee of the College of Medicine / Al-Nahrain University for the present study (clearance No: UNCOMIRB20240511). They were kept in vented plastic cages at the University of Al-Animal Nahrain's Laboratory under regular environmental conditions (12/12 h dark/light cycle, 25°C) [10]. This study investigates the anti-tumor efficacy of N-Benzoyl-3-phenyl isoserine and a vanillin derivative featuring a 1,2,3-triazole ring on Michigan Cancer Foundation-7 (MCF-7) breast cancer cells. This molecule possesses anti-cytokine storm [11] and anti-inflammatory properties; it was synthesized according to the sabbar Omran Z. method [12]. The article will designate the novel chemical compound as the N3 compound; the chemical structure is 3-benzamido-2-(4-((4-formyl-3-methoxyphenoxy)methyl)-1H-1,2,3-triazol-1-yl)-3-phenylpropanoic acid. It was synthesized according to the Sabbar Omran Z. method [12].

Aortic ring assay

Rat aortic ring transplant cultures were created by following the Zhu technique's instructions [13]. We took aortic rings out of male Sprague Dawley rats. The aortas were divided into cross sections of 1-2 mm and repeatedly cleaned with a salt solution that included 2.5 µg/ml of amphotericin B. For each well, 500 µl of 3 mg/ml fibrinogen in serum-free M199 media for development was added, along with 5 µg/ml of aprotinin to prevent fibrinolysis. Ten microliters of thrombin (50 U/ml) in 0.15 M NaCl were applied to every tissue fragment that had been positioned in the center of the hole. 0.5 ml of medium M 199, supplemented with 0.1% ε-aminocaproic acid, 20% heat-inactivated fetal bovine serum (HIFBS), 2.5 µg/ml amphotericin B, 1% L-glutamine, and 60 µg/ml gentamicin, was added to every well once the vessel section had been embedded in the fibrin gels. Tissue culture plates with 48 wells were used for the study (Costar, USA). The N3 compound at the following concentrations: The levels of 200, 100, 50, 25, 12.5, and 6.25 µg/ml among the samples were included in the whole growth medium. The control cultures were administered media containing only the vehicle Dimethyl sulfoxide (DMSO). Cultures were maintained at 37°C for 5 days in a moistened CO2 environment, with the medium being replenished on day 4 [13, 14].

The extent of vascular growth obstruction was evaluated using the Nicosia method [15]. The averaged % of inhibition in relation to the negative control ±SD (standard deviation) was used to assess the regulation of vessel expansion. The concentration that inhibits 50% of proliferating blood vessels, known as $IC_{50,}$ was determined using either the linear regression equation or logarithmic formula for the extraction. Let X stand for the level and Y for the degree of inhibition [16].

Cell culture

Neonatal human dermal fibroblasts (HDFn) and the MCF-7 human breast cancer cell line were obtained from the American Type Culture Collection (ATCC) in Rockville, USA [17]. HDFn cells were cultured in Dulbecco's Modified Eagle's Medium (DMEM), which was supplemented with antibiotics, 10 ng/ml of vascular endothelial growth factor (VEGF), and 10% fetal calf serum (FCS). Human cancer cells were grown in 50 cm^2 flasks (Nunc Brand, Denmark) with 5% CO2 at 37°C. The flasks contained 5 mL of Roswell Park Memorial Institute-1640 Medium (RPMI-1640) (Gibco, USA), supplemented with 10% fetal bovine serum and antibiotics (0.001 g streptomycin and 103 IU penicillin). Human breast cancer cells were employed for a maximum of four passages. Additionally, 0.5 mL of trypsin (Nutricell, Brazil) was included to the culture flasks to dissociate the adherent cell lines. After that, trypsin was deactivated with the extra of 5 mL of RPMI 1640 enriched with 5% fetal bovine serum. Cells were meticulously pipetted to facilitate their dispersion in the fluid. Dimethyl sulfoxide (DMSO) from Sigma was employed to dissolve N3 compound samples before including RPMI at the ultimate level of 100 µg/mL. The cells were exposed to a medium containing DMSO as a negative control [18].

Cytotoxicity assay

Tetrazolium dye (3-[4, 5-dimethylthiazol-2-yl]-2, 5-diphenyltetrazolium bromide [MTT]) was employed in a study to assess the Mosmann Technique's ability to limit cell growth [19]. Every well of a 48-well plate was injected with 1 × 104 MCF-7 and HdFn cells. The cells then underwent incubation for 24 hours at 37°C with 5% CO_2. N3 compound was applied to cells at 70–80% confluence at several levels (200, 100, 50, 25, and 12.5 µg/ml). To make the MTT test, 5 mg/ml was dissolving in phosphate-buffered saline (PBS) and then added to every well. The plates underwent incubation for an extra five-hour period at 37°C after the MTT injection. Following the removal of the supernatant, 200 µL of DMSO was included to fully disintegrate the crystals. To disintegrate the dark blue crystals, the plates were vigorously swirled for a minute at room temperature.

Utilizing a microplate reader (HumaReader HS), the absorption at 570 nm was measured with a standard at 650 nm, which indicates the number of metabolically active cells. By splitting the ratio of feasible cells by 100 (Abs. sample/Abs. control), one may get the proportion of viable cells. This equation was used to assess the cells' vitality. It was altered to display a 100% survival rate for the untreated controls. When the proportion of alive cells drops below 100%, cell death takes place [20]. To assess the development inhibition profile of the N3 molecule, the IC50 was developed, which shows the amount needed to prevent 50% of the development of cells.

RNA extraction and cDNA synthesis

Total cellular RNA was taken out utilizing the TriPure Isolation Reagent (Promega, USA) method specified by the manufacturer. Following treatment with RNase-free DNase (Promega, USA), RNA samples were precipitated with 70% ethanol. The subsequent determination of RNA concentration followed by reverse transcription employing Superscript II (Promega, USA) and an oligo-dT20 primer. The samples were stored at -80°C. Using 1.0 µg of total RNA, complementary DNA (cDNA) was produced in 20 µl of total volume using the PCR technique for 1 hour [21]. The MCF-7 breast cancer cells were cultured at an amount of 1 × 104 cells in the flask. The medium was then changed to a fresh solution that contained five levels of the N3 compound: 12.5, 25, 50, 100, and 200 µg/ml. For sixteen hours, the cells underwent incubation at 37°C with 5% CO_2. The Gas Pak Pouch (Becton Dickinson, Sparks, Md., USA) was used to cultivate the cells in hypoxic circumstances. After then, the purpose of collecting the cells was to extract the RNA. The medium was then aspirated, and Trizol reagent was used to separate total RNA for gene transcription analysis [22].

Gene expression by quantitative Real-time (RT)-polymerase chain reaction (PCR) for (VEGF)

The VEGF gene was the one examined in this investigation [23]. VEGF Quanti-Tect SYBR Green primers were procured from Qiagen, Germany. The VEGF gene primers are CCCACTGAGGAGTCCAACAT (forward) and CAT-ACCTCCCCTGTGCAACT (reverse), while the Glyceraldehyde-3-Phosphate Dehydrogenase (GAPDH) gene, serving as a housekeeping gene, has primers GTCTCCTCTGACTTCAACAGCG (forward) and ACCACCCTGTTGCTGTAGCCAA (reverse). This study utilized GAPDH primers from Invitrogen-USA [24].

Total mRNA expression was measured using the SYBR Green kit and the IQ4 real-time quantitative PCR device (Bio-Rad, USA). The present investigation aimed to assessment the relative VEGF mRNA expression of the breast cancer cell line. 12.5 µl of 1X Go-Taq qPCR Master Mix (Promega, USA), 2.0 µl of complementary DNA, and 2.5 µl of primers comprised the response mixture, which had a total volume of 25 µl. The following settings were used in an iQ5 Cycler (Bio-Rad) to accomplish PCR amplification: 40 cycles of denaturation at 95°C for 15 seconds, annealing at 60°C for 45 seconds, and a break at 72°C for 20 seconds were followed by 3 minutes at 95°C. For 15 seconds, the plate was retained at 80°C. To determine the characteristics of each PCR primer, a melting curve was performed by first lowering the temperature to 55°C and then raising it to 95°C at a rate of 0.5°C per 10 seconds. For every amount of the N3 molecule, the standard curve and cycle threshold were used to evaluate the quantification of gene expression. The fold change in comparison to the untreated cell control was calculated after normalizing the gene expression levels to the standard gene expression. The delta-delta Cycle Threshold (ΔΔCT) approach was used to control the findings using the housekeeping gene (GAPDH) [25].

ADME/Tox profile

The in silico ADME/Tox profile is a beneficial tool for forecasting medication contenders' pharmacological and toxicological characteristics, especially when the preclinical phase [26]. For a comprehensive evaluation of the pharmacokinetic profiles of small compounds, the SwissADME web application (http://www.swissadme.ch/) offers readily available computational methods [27]. For the ADME/Tox online tools SwissADME and pkCSM for pharmacokinetics and pharmacodynamics studies, the molecular structures of the N3 molecule were illustrated applying the simplified molecular-input line-entry system (SMILES) nomenclature (COC1=CC(C=O)=CC=C1CC1=CN(N=N1)C(C(NC(=O) C1=CC=CC=C1)C1=CC=CC=CC=C1)C(O)=O). To describe the ADME/Tox profile, we extracted the key ADME/Tox characteristics from the online resources.

Molecular docking studies

Molecular docking investigations were conducted with the use of the GOLD 2022 program developed by the Cambridge Crystallographic Data Centre (CCDC). The synthesized substances were created to target the AAL993 protein database (PDB: 5EW3), with Axitinib acting as a reference medication. This study used the Protein Data Bank (PDB) as its source for the target proteins. We followed the CCDC-published official GOLD user guide when we ran the docking technique [28]. The active site's pocket was defined as an area of 10 Å. The protein was modified by adding hydrogens, and the tautomerism and ionization states of the residues at the active site were studied. The molecules of water, ligands, cofactors, and superfluous chains were eliminated. Quantification of the docked molecules was done using the PLP (Precise Linear Potential) fitness score. Each docked molecule's intermolecular interactions were captured and recorded [29].

Statistical analysis

The Mean and Standard Deviation (SD) were employed to exhibit the collected data. To compare treatment groups, an

analysis of variance (ANOVA) and a two-tailed Tukey test were employed. At $P < 0.0001$, the mean differences are considered substantial. The IC50 was calculated using non-linear regression evaluation and GraphPad Prism software version 9.0.

Results and Discussion

Anti-angiogenic activity using the ex-vivo rat aorta ring assay

An *ex vivo* rat aortic ring experiment was employed to assess the anti-angiogenic properties of the N3 compound. **Figure 1** illustrates that VEGF-A significantly enhanced the formation of a complex network of microvessels surrounding the aortic rings. Six doses of the N3 compound were utilized, specifically 200, 100, 50, 25, 12.5, and 6.25 µg/ml. The percentage of inhibitions were characterized as mean ± SD as follows: 84%±2.65, 82%±2.08, 68%±2.52, 53%±2.31, 50%±2.08 and 42%±2.08 for the directly above concentration, respectively. Comparing the serial doses to the negative control (DMSO 1%) revealed strong dose-dependent inhibitory effect ($P<0.001$). Blood vessels were enumerated after five days of the experiment, with a sample size of (n=18). The IC_{50} value, derived from the linear regression equation $Y = 13.232\ln(x) + 15.99$, is 13.07 µg/ml. **Figure 2** illustrates the dose-reaction curve of the serial dilution of the N3 compound administered to the rat aorta.

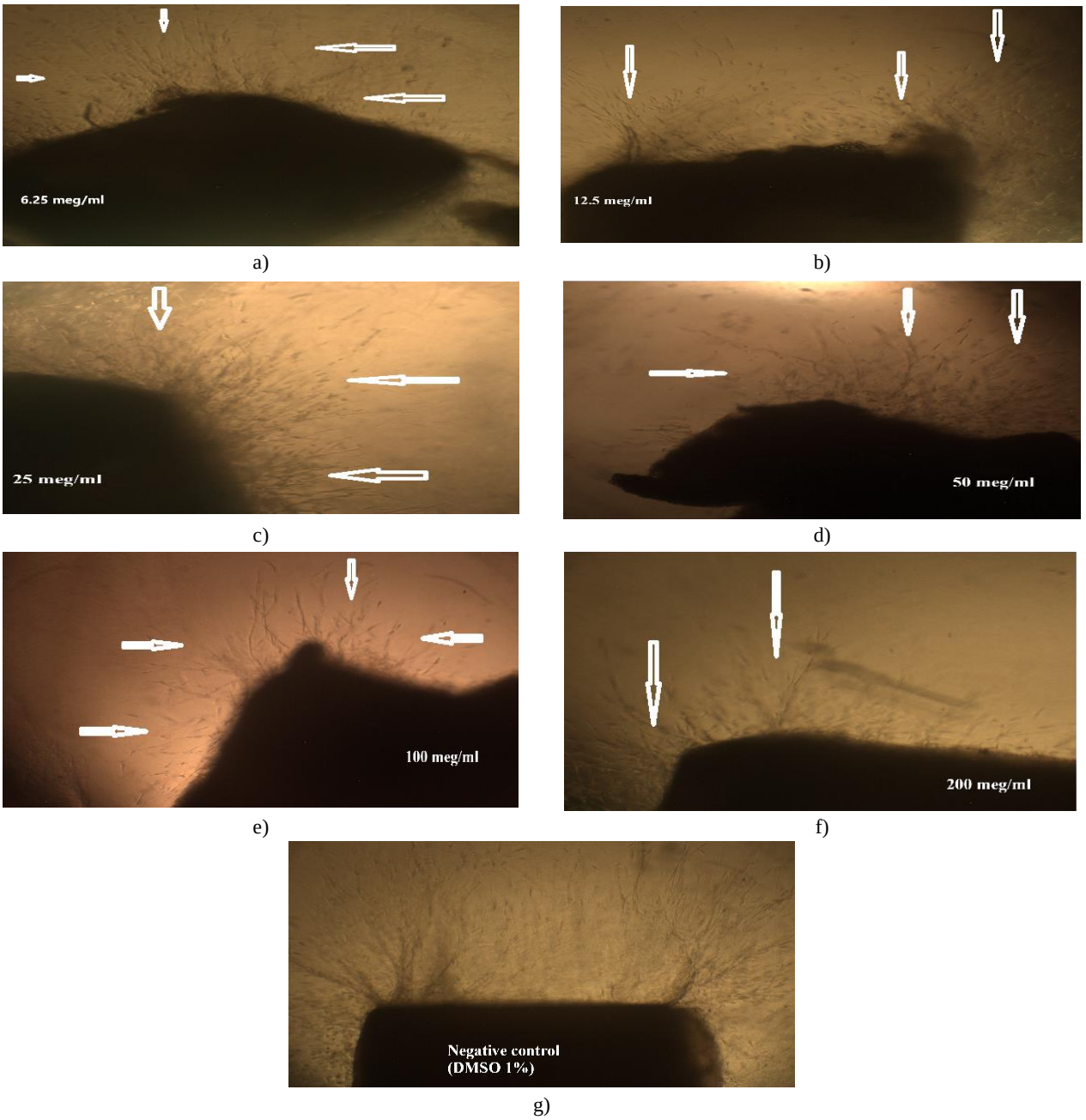

Figure 1. the impact of successive N3 compound levels: a: 200 µg/ml, b: 100 µg/ml, c: 50 µg/ml, d: 25 µg/ml, e: 12.5 µg/ml, f: 6.25 µg/ml, and g: negative control on blood vessel formation in rat aorta rings

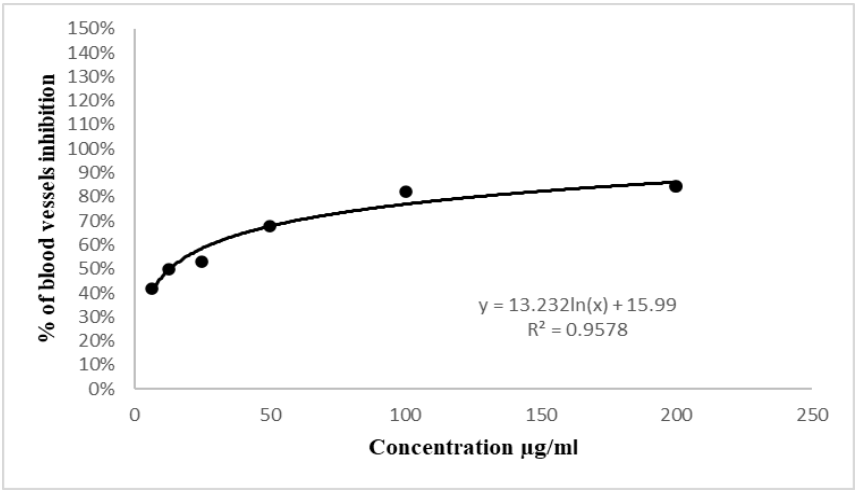

Figure 2. With y representing the percentage of inhibition and x representing the level, this dose-response curve illustrates the inhibitory impact of varying N3 compound levels on the rat aorta ring test.

Cytotoxic effects of the N3 compound using MTT assay

The antitumoral efficacy of the N3 compound was assessed against MCF-7 and HDFn cells utilizing an MTT assay for 24 hours **(Figure 3)**. A indicates that the N3 compound had substantial ($p < 0.0001$) antitumoral efficacy against MCF-7 cells in a dose-dependent manner, with decreased rates of 77.51 ± 0.71%, 65.93 ± 1.36%, 53.01± 2.72%, 40.2±1.68 and 28.7 ± 0.42% for doses of 12.5, 25, 50, 100, and 200 µg/mL, respectively. By comparing with HDFn, the N3 compound treatments were administered at the same doses with decreased rates of 94.75 ± 0.4%, 93.4 ± 0.64%, 88.19± 2.63%, 83.72±1.23 and 71.57±1.51%. The IC_{50} value of 66.85 µg/ml indicates the cytotoxic effect of the chemical on MCF-7 cancer cells, while the IC_{50} for normal HDFn cells is 70.74 µg/ml, as illustrated in **Figure 3b**.

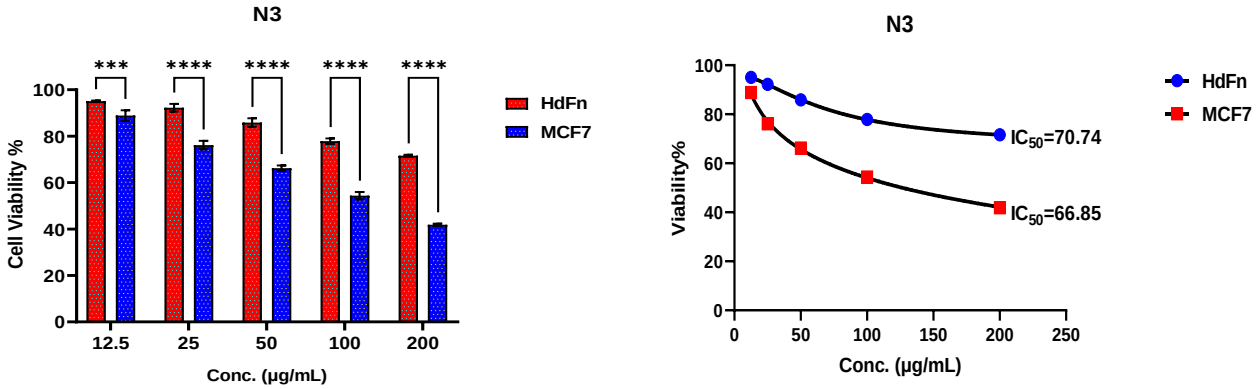

a) b)

Figure 3. The cytotoxic effect of N3 compound on human breast cancer (MCF-7) and neonatal human dermal fibroblasts (HDFn) cells. ***p = 0.0002, ****p <0.0001. a) The inhibitory impact of 12.5, 25, 50, 100, and 200 µg/ml of N3 compound on neonatal human dermal fibroblasts (HDFn) cells and human breast cancer (MCF-7), b) Survival cell curve (mean ± SD%) of MCF-7 and (HDFn) cells following therapy with N3 compound utilizing MTT in vitro assay at 37 °C, 5% CO2 for 24 h.

Gene expression of vascular endothelial growth factors (VEGF) for Breast cancer cells (MCF-7) using RT-PCR and the activity of the N3 compound on VEGF gene expression

The N3 compound decreased the transcription levels of VEGFR-2 in MCF-7 cell cultures. To investigate the impact of hypoxia on VEGF mRNA expression degrees, RT-quantitative PCR was employed to detect mRNA levels in MCF-7 cells grown for 48 hours with varying doses of N3 compound. **Figure 4** depicts the dose-response relationship of the N3 compound on VEGF gene expression depending on ΔΔCt method, demonstrating a reduction in value in contrast to the control. Moreover, there was no substantial alteration in VEGF mRNA expression after treatment with N3 compound concentrations (25, 50, and 100 µg/mL), which resulted in reductions in VEGFR-2 transcription with P-values of 0.5288, >0.9999, and 0.7168, respectively, in comparison to the control. The expression of VEGF mRNA was considerably elevated by treatment with 12.5 µg/mL of N3

compound (P-value 0.0097), and a notable alteration in VEGF mRNA expression was seen following treatment with 200 µg/mL of N3 compound (P-value < 0.0001) in contrast to the control.

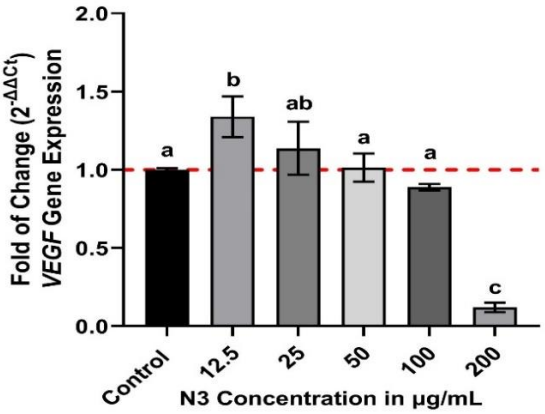

Figure 4. Impact of the N3 compound on VEGF gene expression for Breast cancer cells (MCF-7) using RT-PCR, Fold of gene expression of VEGF gene after exposure to different concentrations of N3 compound depending on ΔΔCt method. (a, ab) p > 0.0001, (b,c) p < 0.0001

Assessment of pharmacokinetics and the target proteins

Absorption was anticipated based on solubility and lipophilicity. Lipophilicity was estimated employing the SwissADME Consensus Log Po/w descriptor to forecast the logarithm of the n-octanol/water partition parameter. The anticipated value of Consensus log $P_{o/w}$ for the N3 compound is 2.96. The water solubility was assessed utilizing the Silicos *IT* Log_{Sw} descriptor from Swiss ADME. The anticipated Log $_{Sw}$ values for our compound were -7.38. The Swiss ADME Log_{Sw} scale indicates that the N3 compound is considered weakly soluble if its values are below −6. (Log Sw scale: insoluble < -10 < poorly < -6 < Moderately < -4 < soluble < -2 < very < 0 < Highly). In the distribution, the glycoprotein P (P-gp) substrate and blood-brain barrier (BBB) permeable were employed. Utilizing Swiss ADME, metabolism was assessed with an emphasis on the suppression of the P450 superfamily's major cytochromes (CYP), specifically CYP3A4, CYP1A2, CYP2C9, CYP2D6, and CYP2C19. One of the main mechanisms for drug-drug encounters is the inhibition of CYP enzymes, which occurs when medications compete for the same enzyme docking site. Drug-likeness characteristics selected by Lipinski were calculated utilizing Swiss ADME. Excretion mainly entails renal and hepatic clearance and is linked to bioavailability.

Molecular docking

The obtained docking scores are expressed by Preciece Linearwise potential (PLP) fit-ness, which forecasts how well the docked chemical will tie to the protein. The scoring function is based on PLP Fitness, which models the steric and clashing interactions between the ligand and the protein. **Table 1** shows PLP fitness and bonded Interactions. Axitinib and the N3 molecule served as reference medications.

Table 1. Molecular docking score of the N3 compound in comparison to reference drug Axitinib

Compounds	PLP fitness	Interactions	3D structure
N3 compound	81.783	GLU 885 (HB), VAL 899 (VDW)	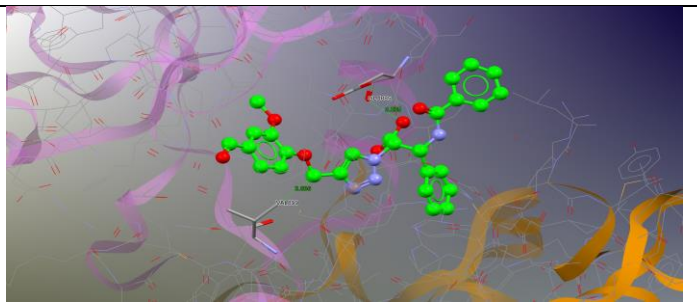
Axitinib	78.748	ILE 1025 (HB)	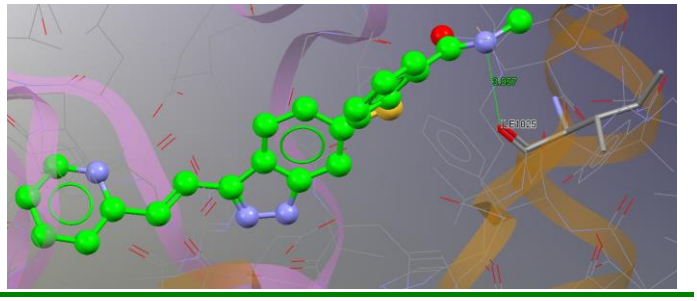

HB: Hydrogen bond, VDW: Van Der Waals.

The leading cause of death is still cancer, with a rising incidence observed globally over the past few years. The predominant cause of cancer-related fatalities is metastasis. Consequently, the critical function of angiogenesis in tumor metastasis reduces it to a viable target for the development of anti-tumor pharmaceuticals [30]. Targeting tumor vasculature promotes anti-cancer immunity and increases the efficacy of chemotherapy. At present, anti-angiogenic medication is

employed clinically in the adjuvant context for cancer patients [31]. Although the availability of additional transmission pathways implicated in angiogenesis, efforts to develop novel anti-angiogenic drugs have been focused on blocking VEGF/VEGFR signaling, a crucial manager [32].

The rat aorta ring assay is a prevalent method for investigating angiogenesis and its causes because of its consistency, simplicity, cost-effectiveness, and strong association with *in vivo* assays [3]. This work aimed to investigate the anti-angiogenic and antiproliferative effects of the N3 compound, which were assessed using the rat aorta rings, revealing a considerable restriction of blood vessel expansion in contrast to the adverse control. A dose-response relationship denotes the alteration in the magnitude of a drug's action as the dosage fluctuates. This instance examines the N3 compound, where the relationship is established by evaluating the impact of varying compound concentrations on the contraction or relaxation of vascular tissues, namely rat aorta rings. To determine the level at which 50% of the blood vessels are inhibited, a dose-response curve has been created [33]. With an IC50 of 13.07 µg/ml, the dose-response research of the N3 compound employing the rat aorta ring testing showed substantial dose-dependent inhibition. This is within the legal scale, according to Nassar, who noted that the threshold level of a herbal extract considered secure in the procedure of angiogenesis is 20 µg/ml [34]. The N3 molecule may have anti-angiogenic properties by blocking VEGF-A/VEGFR-2 and VEGF-C/VEGFR-3 signaling. The main VEGF signal mediator in angiogenesis is VEGFR-2. The linking of the VEGF-A to VEGFR-2 induces dimerization, subsequently promotes phosphorylation of particular tyrosine residues, and activation of angiogenic signaling [31].

Breast cancer, which has high recurring rates, is the most frequent cancer in women and an essential reason for mortality for women worldwide [35]. Hypoxic microenvironments are present in 25–40% of offensive breast cancer cases, indicating that breast cancer is sensitive to hypoxia [36]. Breast cancer patients' survival rate may be negatively impacted by intra-tumoral hypoxia, which may promote the enlargement of breast cancer cells and their migration through the epithelial-mesenchymal transition [36]. The major activated factors are hypoxia-inducible factors (HIFs), which subsequently upregulate several pro-angiogenic genes either directly or indirectly [33]. Breast cancer is linked with increased expression of HIF-1α and its target genes [37]. VEGF regulates various cellular activities, including mitosis, permeability, and vasoconstrictor tension. VEGF expression is intricately linked to tumor angiogenesis and lymphangiogenesis in breast cancer [38]. VEGF is a aimed gene of HIF-1, and the HIF-1 transcriptional complicated can stimulate the production of VEGF and elicit the associated biological consequences [39]. The N3 compound's anticancer efficacy was assessed using human breast cancer MCF-7 cells. This cell line was selected for *in vitro* experiments based on NCI's five dose-response analysis methods [40]. The neonatal human dermal fibroblasts (HDFn) cell line was utilized as a noncancerous model to assess the particular anti-cancer efficacy of the N3 compound. The MTT cytotoxicity assay findings show that, within the dosage range employed in the study, the N3 compound exhibited cytotoxic action in breast cancer cell lines **(Figure 3)**. The anticancer efficacy is shown by an IC_{50} value (µg/mL). An IC_{50} value below 100 signifies a substance with anticancer properties. An IC_{50} value ranging from 100 to 300 signifies inadequate anticancer efficacy, whereas an IC_{50} over 300 indicates an inactive compound [41, 42]. The findings revealed IC50 values of 70.74 µg/mL for HDFn and 66.85 µg/mL for MCF-7. This discovery indicates that the N3 compound could be developed as an anticancer drug. The findings demonstrate considerable antiproliferative capacity of the N3 compound towards MCF-7 breast cancer cells.

Quantifying gene expression levels has become a core procedure in the majority of molecular biology laboratories. Quantifying cellular RNA measures the level of gene expression. The quantitative measure for real-time PCR is the threshold cycle (CT). CT value demonstrates an inverse relationship with the amplicon quantity in the reaction; thus, a lower CT indicates a greater amplicon concentration [25]. The examination of VEGF gene expression in the present investigation revealed that breast cancer (MCF-7) cells treated with the N3 compound demonstrated a reduction in VEGF gene expression (down-regulation) compared to control cells at doses of 25, 50, and 100 µg/mL; however, this decrease was not statistically significant. Additionally, an increase in VEGF gene expression (up-regulation) was observed at a dose of 12.5 µg/mL. In contrast, considerable variability was seen at 200 µg/mL doses regarding their impact on VEGF gene expression and showed effectiveness in inhibiting gene expression. Angiogenesis is essential for metastasis and advancement of breast cancer. Consequently, growth factors and indicators that govern angiogenesis and tumor advancement are critical targets for the formulation of tailored molecular treatments [43]. The qRT-PCR results indicated that the N3 chemical inhibits VEGF expression in a concentration-dependent manner in the MCF-7 cell line.

To determine the ADME/Tox-related parameters for the N3 molecule, we used the SwissADME and pkCSM pharmacokinetics servers. Fast and accurate ADME/Tox property predictions are made possible by the pkCSM pharmacokinetics server. It was created by cautiously picking established processes and data sets from the literature [26]. The standard indicator of lipophilicity is the partition coefficient (log Po/w) between n-octanol and water; the N3 compound demonstrated strong lipophilicity with a consensual log Po/w value of 2.96. Because this physicochemical property is so crucial for pharmacokinetic medication production, it has its own domain in SwissADME [44]. The skin permeability coefficient (Kp) is calculated using a multiple linear regression model. Lipophilicity and molecule size are linearly correlated with Kp ($R^2 = 0.67$). A lower log Kp value (measured in cm/s) indicates that the N3 compound has less skin permeability. The log Kp of the N3 compound is -6.69, which leads to reduced skin permeability. P-glycoprotein is an ATP-dependent efflux pump present in multiple human organs. N3 compound was anticipated to be substrates of P-glycoprotein. Knowledge of the interaction between chemicals and cytochromes P450 (CYP) is also crucial.

This isoenzyme superfamily is crucial for medication clearance via metabolic biotransformation [45]. CYP and P-gp are proposed to metabolize small compounds, enhancing tissue and organism defence collaboratively. According to different authors, between 50 and 90 percent of pharmaceutical substances are substrates of the five main isoforms of CYP3A4, CYP1A2, CYP2C9, CYP2D6, and CYP2C19 [46]. Decreased clearance and buildup of the drug or its metabolites result in toxicity or other negative consequences, and the inhibition of these isoenzymes plays a major role in pharmacokinetics-related drug-drug interactions [47]. When nascent substances were effectively progressed to be evaluated as oral medication applicants, their structural or physicochemical features were analyzed to identify their drug-likeness. Lipinski's rule of five states that there is a high chance of optimum absorbing or penetrating when the molecular weight (MW) is below 500 Da, the number of hydrogen bond donors (HBDs) is fewer than 5, and the logP is below five. Investigations using molecular docking have shown that there are fewer than ten hydrogen bond acceptors (HBAs) [48]. The N3 compound possesses all necessary features without contravening Lipinski's rule of five, and it is expected to exhibit substantial absorption and cellular permeability. Elevated oral bioavailability is a crucial factor for the introduction of biologically active compounds into the therapeutic market. The N3 compound has a bioavailability of 0.56, representing a moderate value. Oral bioavailability can be anticipated by analyzing the molecular characteristics, such as low polar surface area, complete hydrogen bonding, diminished molecular flexibility, and effective intestinal absorption [49]. ADME parameters, pharmacokinetic profile, and drug-likeness of the N3 compound were anticipated utilizing the free web usage SwissADME (http://www.swissadme.ch/index.php) developed by the Swiss Institute of Bioinformatics.

Molecular docking simulations are computational methods that evaluate the interaction of a molecule with its target. The literature widely employs these investigations to assess the *in-silico* activities of a synthesized chemical [29]. The VEGF2 receptors experience autophosphorylation at the tyrosine kinase domain upon VEGF binding, initiating downstream mechanisms that facilitate vascular proliferation and migration [50]. Axitinib, an FDA-approved angiogenic inhibitor, is a selective VEGFR inhibitor characterized by fewer adverse responses and improved safety. Consequently, axitinib serves as a reference compound for identifying possible VEGFR-2 inhibitors in our research [51]. Theoretically, the new ligand possesses high pharmacological activity and higher potency in comparison with Axitnib due to the addition of a carboxylic acid functional group, which is ionized in physiological PH to carboxylate anion, thus forming a new ionic bond with the active site of VEGF2 and addition of new aromatic functional group that is lead to forming a new hydrophobic bond with VEGF2.

Conclusion

Our results reveal that the phenyl isoserine derivative exerts an inhibitory impact on the expansion of the MCF-7 breast cancer cell line as opposed to the command group. The anti-cancer properties of the phenyl isoserine derivative may be partially attributed to its involvement in angiogenesis, invasion, and metastasis via suppressing angiogenesis in the *ex vivo* rat aorta assessment and the downregulation of VEGF in breast cancer cells. The findings indicate that the phenyl isoserine derivative may be regarded as a viable anti-cancer option for novel medication development in cancer therapy. Summarise the main findings of the study.

Animal experiments

Sprague Dawley rats were housed under conventional living conditions for the one-week acclimatization period, with a 12-hour light/dark cycle, and they had unrestricted access to clean water and standard feed pellets. To ensure deep anaesthesia and the absence of responsiveness to pain, animals were given intraperitoneal injections of ketamine (80 mg/kg) and xylazine (10 mg/kg) before the aortic ring experiments.

Acknowledgments: The authors express their gratitude to the College of Medicine, Al-Nahrain University, for their essential support in enabling this research. The establishment of a fully equipped laboratory and the promotion of scientific inquiry significantly facilitated the effective completion of this investigation. Your commitment to promoting research excellence is greatly valued.

Conflict of interest: None

Financial support: None

Ethics statement: All experimental procedures complied with the standards set by the College of Medicine / Al-Nahrain University Committee for Animal Care and received approval from The Research Ethical Committee of the College of Medicine / Al-Nahrain University for the present study (clearance No: UNCOMIRB20240511).

References

[1] Gupta GP, Massagué J. Cancer metastasis: building a framework. Cell. 2006;127(4):679-95. doi:10.1016/j.cell.2006.11.001

[2] Güner A, Polatli E, Akkan T, Bektaş H, Albay C. Anticancer and antiangiogenesis activities of novel synthesized 2-substituted benzimidazoles molecules. Turk J Chem. 2019;43(5):1270-89. doi:10.3906/kim-1904-46

[3] Abu-Raghif AR, Sahib HB, Hanoon MM. Anti-angiogenic activity of Zizyphus spinachristi leaves extracts. Int J Pharm Sci Rev Res. 2015;35(1):32.

[4] Mohammed MK, Al-Shuhaib Z, Al-Shawi AAA. Synthesis, characterization and cytotoxicity appraisal of original 1, 2, 3-Triazole derivatives, against breast cancer cell lines

(MDA-MB-231). Mediterr J Chem. 2019;9(4):305-10. doi:10.13171/mjc941911161021mkm

[5] Ruddarraju RR, Murugulla AC, Kotla R, Chandra Babu Tirumalasetty M, Wudayagiri R, Donthabakthuni S, et al. Design, synthesis, anticancer, antimicrobial activities and molecular docking studies of theophylline containing acetylenes and theophylline containing 1,2,3-triazoles with variant nucleoside derivatives. Eur J Med Chem. 2016;123:379-96. doi:10.1016/j.ejmech.2016.07.024

[6] Savaş B, Öztürk T, Meyvacı E, Hazer B. Synthesis and characterization of comb-type graft copolymers by redox polymerization and "click" chemistry method. SN Appl Sci. 2020;2(2):181. doi:10.1007/s42452-020-1985-z

[7] Malah T El, Nour HF, Satti AAE, Hemdan BA, El-Sayed WA. Design, synthesis, and antimicrobial activities of 1,2,3-triazole glycoside clickamers. Molecules. 2020;25(4):790. doi:10.3390/molecules25040790

[8] Kollaschinski M, Sobotta J, Schalk A, Frischmuth T, Graf B, Serdjukow S. Efficient DNA click reaction replaces enzymatic ligation. Bioconjug Chem. 2020;31(3):507-12. doi:10.1021/acs.bioconjchem.9b00805

[9] Samarasimhareddy M, Shamir M, Shalev DE, Hurevich M, Friedler A. A rapid and efficient building block approach for click cyclization of peptoids. Front Chem. 2020;8:405. doi:10.3389/fchem.2020.00405

[10] Alhashem G, Raghif ARA, Abbas AA. The effect of liraglutide on biochemical markers of bone turnover in rats treated by dexamethasone. Int J Drug Deliv Technol. 2022;12:598-602. doi:10.25258/ijddt.12.2.23

[11] Abed Mansoor AF, Abu Raghif AR. Attenuated effects of rivastigmine in induced cytokine storm in mice. J Emerg. Med Trauma Acute Care. 2022;2022(3):12. doi:10.5339/jemtac.2022.ismc.12

[12] Omran Z sabbar, Sahib HB, Radhi AJ, Ali NM. In silico Design, and in vivo evaluation of synthesized phenyl isoserine derivative and used as anticytokine storm. Egypt J Chem. 2023;66(5):151-9. doi:10.21608/EJCHEM.2022.144346.6319

[13] Zhu WH, Guo X, Villaschi S, Nicosia RF. Regulation of vascular growth and regression by matrix metalloproteinases in the rat aorta model of angiogenesis. Lab Invest. 2000;80(4):545-55. doi:10.1038/labinvest.3780060

[14] Sahib HB. The anti-angiogenic and anti-proliferative activity of methyl hydroxychalcone. Asian Pac J Cancer Prev. 2022;23(6):2071-7. doi:10.31557/APJCP.2022.23.6.2071

[15] Nicosia RF, Lin YJ, Hazelton D, Qian X. Endogenous regulation of angiogenesis in the rat aorta model. Role of vascular endothelial growth factor. Am J Pathol. 1997;151(5):1379.

[16] Stiffey-Wilusz J, Boice JA, Ronan J, Fletcher AM, Anderson MS. An ex vivo angiogenesis assay utilizing commercial porcine carotidartery: modification of the rat aortic ring assay. Angiogenesis. 2001;4:3-9. doi:10.1023/A:1016604327305

[17] Sieuwerts AM, Klijn JGM, Peters HA, Foekens JA. The MTT tetrazolium salt assay scrutinized: how to use this assay reliably to measure metabolic activity of cell cultures in vitro for the assessment of growth characteristics, IC50-values and cell survival. Clin Chem Lab Med. 1995;33(11):813-24. doi:10.1515/cclm.1995.33.11.813

[18] Al-Rawi SS, Ibrahim AH, Hamde MA, Babu D, Nazari M, Kadir MOA, et al. Antiangiogenic and anticancer potential of supercritical fluid extracts from nutmeg seeds; In vitro, Ex vivo and In silico studies. J Angiother. 2023;7(1). doi:10.25163/angiotherapy.719371

[19] Mosmann T. Rapid colorimetric assay for cellular growth and survival: application to proliferation and cytotoxicity assays. J Immunol Methods. 1983;65(1-2):55-63. doi:10.1016/0022-1759(83)90303-4

[20] Patel V, Joshi U, Joshi A, Upadhyay TK, Al-Keridis LA, Saeed M. Cytotoxicity analysis for the hydroxyl functionalized MWCNT reinforced PMMA nanocomposites in oral squamous carcinoma (KB) cells. Polymers. 2023;15(5):1192. doi:10.3390/polym15051192

[21] Juskowiak B, Bogacz A, Wolek M, Kaminski A, Uzar I, Seremak-Mrozikiewicz A, et al. Expression profiling of genes modulated by rosmarinic acid (RA) in MCF-7 breast cancer cells. Ginekol Pol. 2018;89(10):541-5. doi:10.5603/GP.a2018.0092

[22] Andergassen U, Kölbl AC, Mahner S, Jeschke U. Real-time RT-PCR systems for CTC detection from blood samples of breast cancer and gynaecological tumour patients (Review). Oncol Rep. 2016;35(4):1905-15. doi:10.3892/or.2016.4608

[23] Adams G. A beginner's guide to RT-PCR, qPCR and RT-qPCR. Biochem. 2020;42(3):48-53. doi:10.1042/BIO20200034

[24] Accomando WP, Wiencke JK, Houseman EA, Nelson HH, Kelsey KT. Quantitative reconstruction of leukocyte subsets using DNA methylation. Genome Biol. 2014;15:1-2. doi:10.1186/gb-2014-15-3-r50

[25] Livak KJ, Schmittgen TD. Analysis of relative gene expression data using real-tim e quantitative PCR and the 2 C T method. Methods. 2001;25(4):402-8.

[26] Durán-Iturbide NA, Díaz-Eufracio BI, Medina-Franco JL. *In Silico* ADME/Tox profiling of natural products: a focus on BIOFACQUIM. ACS Omega. 2020;5(26):16076-84. doi:10.1021/acsomega.0c01581

[27] Daina A, Michielin O, Zoete V. SwissADME: a free web tool to evaluate pharmacokinetics, drug-likeness and medicinal chemistry friendliness of small molecules. Sci Rep. 2017;7(1):42717. doi:10.1038/srep42717

[28] Ferrence GM, Tovee CA, Holgate SJW, Johnson NT, Lightfoot MP, Nowakowska-Orzechowska KL, et al. CSD communications of the cambridge structural database. IUCrJ. 2023;10(1):6-15. doi:10.1107/S2052252522010545

[29] Hussein SS, Ali KF, Al-Saady FA. Synthesis, characterization, molecular docking, and preliminary

antimicrobial evaluation of thiazolidinone derivatives. Pal Med Pharm J. 2024;9(2):6. doi:10.59049/2790-0231.1152

[30] Lugano R, Ramachandran M, Dimberg A. Tumor angiogenesis: causes, consequences, challenges and opportunities. Cell Mol Life Sci. 2020;77:1745-70. doi:10.1007/s00018-019-03351-7

[31] Hsu MJ, Chen HK, Chen CY, Lien JC, Gao JY, Huang YH, et al. Anti-angiogenetic and anti-lymphangiogenic effects of a novel 2-aminobenzimidazole derivative, MFB. Front Oncol. 2022;12:862326. doi:10.3389/fonc.2022.862326

[32] Momeny M, Alishahi Z, Eyvani H, Esmaeili F, Zaghal A, Ghaffari P, et al. Anti-tumor activity of cediranib, a pan-vascular endothelial growth factor receptor inhibitor, in pancreatic ductal adenocarcinoma cells. Cell Oncol. 2020;43:81-93. doi:10.1007/s13402-019-00473-9

[33] Raghif AR. The anti-angiogenic activity of P-hydroxy chalcone. Int J Pharm Sci Rev. 2016;37:117-21.

[34] Nassar ZD, Aisha AFA, Ahamed MBK, Ismail Z, Abu-Salah KM, Alrokayan SA, et al. Antiangiogenic properties of Koetjapic acid, a natural triterpene isolated from Sandoricum koetjaoe Merr. Cancer Cell Int. 2011;11:1-8. doi:10.1186/1475-2867-11-12

[35] Rogulski L, Oszukowski P. Epidemiological models for breast cancer risk estimation. Ginekol Pol. 2011;82(6).

[36] Lundgren K, Holm C, Landberg G. Hypoxia and breast cancer: prognostic and therapeutic implications. Cell Mol Life Sci. 2007;64(24):3233-47. doi:10.1007/s00018-007-7390-6

[37] Li Q, Ma R, Zhang M. CoCl2 increases the expression of hypoxic markers HIF-1α, VEGF and CXCR4 in breast cancer MCF-7 cells. Oncol Lett. 2018;15(1):1119-24. doi:10.3892/ol.2017.7369

[38] Komatsu DE, Hadjiargyrou M. Activation of the transcription factor HIF-1 and its target genes, VEGF, HO-1, iNOS, during fracture repair. Bone. 2004;34(4):680-8. doi:10.1016/j.bone.2003.12.024

[39] Dong X, Wang YS, Dou GR, Hou HY, Shi YY, Zhang R, et al. Influence of dll4 via hif-1α-vegf signaling on the angiogenesis of choroidal neovascularization under hypoxic conditions. PLoS One. 2011;6(4):e18481. doi:10.1371/journal.pone.0018481

[40] Monks A, Scudiero D, Skehan P, Shoemaker R, Paull K, Vistica D, et al. Feasibility of a high-flux anticancer drug screen using a diverse panel of cultured human tumor cell lines. J Natl Cancer Inst. 1991;83(11):757-66.

[41] Al-Douh MH, Sahib HB, Osman H, Hamid SA, Salhimi SM. Anti-proliferation effects of benzimidazole derivatives on HCT-116 colon cancer and MCF-7 breast cancer cell lines. Asian Pac J Cancer Prev. 2012;13(8):4075-9. doi:10.7314/APJCP.2012.13.8.4075

[42] Arsianti AA, Fadilah F, Fatmawaty Y, Wibisono LK, Kusmardi S, Azizah NN, et al. Phytochemical composition and anticancer activity of seaweeds Ulva lactuca and Eucheuma cottonii against breast MCF-7 and colon HCT-116 cells. Asian J Pharm Clin Res. 2016;9(6):115-9. doi:10.22159/ajpcr.2016.v9i6.13798

[43] Deryugina EI, Quigley JP. Tumor angiogenesis: MMP-mediated induction of intravasation- and metastasis-sustaining neovasculature. Matrix Biol. 2015;44:94-112. doi:10.1016/j.matbio.2015.04.004

[44] Arnott JA, Planey SL. The influence of lipophilicity in drug discovery and design. Expert Opin Drug Discov. 2012;7(10):863-75. doi:10.1517/17460441.2012.714363

[45] Testa B, Krämer SD. The biochemistry of drug metabolism - An introduction Part 1. Principles and overview. Chem Biodivers. 2006;3(10):1053-101. doi:10.1002/cbdv.200690111

[46] Di L. The role of drug metabolizing enzymes in clearance. Expert Opin Drug Metab Toxicol. 2014;10(3):379-93. doi:10.1517/17425255.2014.876006

[47] Kirchmair J, Göller AH, Lang D, Kunze J, Testa B, Wilson ID, et al. Predicting drug metabolism: experiment and/or computation? Nat Rev Drug Discov. 2015;14(6):387-404. doi:10.1038/nrd4581

[48] Lipinski CA. Lead- and drug-like compounds: the rule-of-five revolution. Drug Discov Today Technol. 2004;1(4):337-41. doi:10.1016/j.ddtec.2004.11.007

[49] Refsgaard HHF, Jensen BF, Brockhoff PB, Padkjær SB, Guldbrandt M, Christensen MS. In silico prediction of membrane permeability from calculated molecular parameters. J Med Chem. 2005;48(3):805-11. doi:10.1021/jm049661n

[50] Bold G, Schnell C, Furet P, McSheehy P, Brüggen J, Mestan J, et al. A novel potent oral series of VEGFR2 inhibitors abrogate tumor growth by inhibiting angiogenesis. J Med Chem. 2016;59(1)132-46. doi:10.1021/acs.jmedchem.5b01582

[51] Bao J, Zhou N, Luo K, Zhang W, Li X, Wu C, et al. In silico discovery of potential VEGFR-2 inhibitors from natural derivatives for anti-angiogenesis therapy. Int J Mol Sci. 2014;15(9):15994-6011. doi:10.3390/ijms150915994